

# Sensitivity at the degenerate points of energy levels in a quantum system with nonintegrable perturbation

Yingxin Jin and Kaifen He

Key Laboratory in University for Radiation Beam Technology and Materials Modification, Beijing Normal University, Beijing 100875, China;

Institute of Low Energy Nuclear Physics, Beijing Normal University, Beijing 100875, China;

Beijing Radiation Center, Beijing 100875, China;

and CCAST (World Laboratory), P.O. Box 8730, Beijing 100080, China

(Received 25 June 2000; published 18 May 2001)

The behavior of quantum states and observables of a quasi-integrable quantum system is studied. Sensitivity of the quantum states and nonperiodicity of the average value of observables at the degenerate points of energy levels are observed. The behavior demonstrates the quantum properties corresponding to the classical resonant tori with rational frequency ratio, where the global structure is easily destroyed by a small perturbation. Our result is helpful for further understanding the avoided crossing in hard chaotic quantum systems.

DOI: 10.1103/PhysRevE.63.066210

PACS number(s): 05.45.Mt, 03.65.-w

## I. INTRODUCTION

In the study of quantum chaos, the behavior relevant to energy levels, e.g., the different types of unfolded energy spectra, the spectrum rigidity, etc., is usually considered as the criterion for regular and chaotic motion [1–3,8]. Moreover, the avoided crossing of energy levels is widely accepted as a signature of quantum chaotic motion, especially for hard chaotic systems. In these cases, if a certain parameter of the Hamiltonian is adjusted, the energy levels may vary accordingly; the most miraculous phenomenon is that, with changing parameter, two energy levels may draw nearer, then repel each other, and separate further, as if there exists a hidden repelling force preventing the degeneracy from occurring.

It is well known that, quasi-integrable (i.e., soft chaotic) systems behave intermediately between integrable and totally chaotic ones; a transition from regular to chaotic motion can be observed in these systems. Thus, investigation of the transition process in such systems would be helpful for us to understand the avoided crossing of energy levels in hard chaotic systems.

The transition process can be described as the following. For an originally integrable Hamiltonian system, degeneracies of energy levels can easily take place due to the symmetry of the system; as one of the parameters change, different energy levels may intersect with each other, and the intersecting points are just the degeneracy points of energy levels. If a nonintegrable perturbation is added to the system, the system symmetry is partly destroyed; as a result, some of the degeneracy points are split, and the behavior similar to that of avoided crossing can be observed. As the perturbation strength increases further, the symmetry may be totally destroyed and the degeneracy of energy levels becomes rare, which is rightfully the avoided crossing case.

From the above descriptions, one can infer that the behavior of energy levels at degeneracy points is more crucial than those at the other part of the energy spectra. We need to point out that these degeneracy points are usually related to

the sensitivity of the system. That is, the properties of the system are more sensitive to external perturbation at these points. It can be seen, with semiclassical analysis, that the sensitivity behavior corresponds to the destruction of classical resonant tori.

Recently Xu *et al.* [3,4] has pointed out that overlaps of many avoided crossings at one point can be seen as a signature of quantum chaotic motion, which is the quantum counterpart of classical resonance overlaps. This shows that the behavior of a quantum system at degeneracy points as well as avoided crossings can still be an important topic for further study. Moreover, the phenomena similar to avoided crossing can also be observed in the eigenvalue problems of different wave systems that are beyond the scope of quantum mechanics [6,5,7]. Better understanding of the quantum-mechanical case is also helpful for elucidating the common character in these systems [8–20].

The present paper is organized as follows. In Sec. II we propose a model system with the unperturbed Hamiltonian displaying energy degeneracies; it is shown that the degeneracy points correspond to the classical resonance tori, and are sensitive to perturbation. As a comparison, in Sec. III, the trajectories of observables and their power spectra near the degeneracy points are calculated. Section IV is a discussion, the nonlinear effect in the observables is pointed out.

## II. SENSITIVITY AT DEGENERATE POINTS

To investigate the behavior at the degeneracy points of energy levels, we first need to adopt an integrable model in which the intersection of different energy levels can be observed explicitly. The unperturbed integrable Hamiltonian we consider is

$$H_0(\mu) = H^0 + \mu U = \frac{1}{2}(p_1^2 + x_1^2 + p_2^2 + x_2^2) - \mu x_1 x_2, \quad (1)$$

where  $H^0 = \frac{1}{2}(p_1^2 + p_2^2 + x_1^2 + x_2^2)$ , is the Hamiltonian of a two-dimensional (2D) harmonic oscillator,  $U = -x_1 x_2$ , and  $\mu$  is an adjustable parameter. Here we suppose that the mass of oscillator  $m$ , the angular frequency  $\omega$ , and the Planck's con-

stant  $\hbar$  are equal, i.e.,  $m = \omega = \hbar = 1$ . With this choice of units, the classical and quantum-mechanical quantities behave at the same scale and can be easily compared. Integrability of the model can be proved as follows. By taking

$$\xi_1 = \frac{1}{\sqrt{2}}(x_1 + x_2), \quad \xi_2 = \frac{1}{\sqrt{2}}(x_1 - x_2), \quad (2)$$

and

$$\pi_1 = \frac{1}{\sqrt{2}}(p_1 + p_2), \quad \pi_2 = \frac{1}{\sqrt{2}}(p_1 - p_2), \quad (3)$$

the above relation can be seen as a canonical transform and  $\xi_1, \xi_2; \pi_1, \pi_2$  represents the new variables of coordinates and momenta. Hence we have  $[\xi_1, \pi_1] = [\xi_2, \pi_2] = i(\hbar = 1)$  and the Hamiltonian  $H_0(\mu)$  is transformed into

$$H_0(\mu) = \frac{1}{2}[\pi_1^2 + (1 - \mu)\xi_1^2] + \frac{1}{2}[\pi_2^2 + (1 + \mu)\xi_2^2]. \quad (4)$$

It can be easily seen that this is another 2D harmonic oscillator, which is surely an integrable system. The expression of energy levels can be obtained analytically:

$$E_{m,n} = (m + \frac{1}{2})\sqrt{1 - \mu} + (n + \frac{1}{2})\sqrt{1 + \mu}, \quad (5)$$

$$m, n = 0, 1, 2, \dots$$

To demonstrate the sensitivity, we introduce a nonintegrable perturbation  $\lambda V$ :

$$\lambda V = \lambda(x_1^2 x_2 - \frac{1}{3}x_2^3), \quad (6)$$

which is the external perturbation of Hénon-Heiles oscillator. The strength of perturbation is determined by parameter  $\lambda$ , hence the total Hamiltonian has the following form:

$$H = H_0(\mu) + \lambda V = H^0 + \mu U + \lambda V. \quad (7)$$

To perform the numerical calculation, the representation of a 2D harmonic oscillator is adopted. The Hilbert space is spanned by the eigenstates of the Hamiltonian  $H^0 = \frac{1}{2}(p_1^2 + p_2^2 + x_1^2 + x_2^2)$ , which are

$$\{|m, n\rangle = |m\rangle \otimes |n\rangle; m, n = 0, 1, 2, \dots\}. \quad (8)$$

$|m, n\rangle, |m\rangle$  and  $|n\rangle$  are the eigenstates satisfying the following equations:

$$H^0|m, n\rangle = \frac{1}{2}(p_1^2 + x_1^2 + p_2^2 + x_2^2)|m, n\rangle = (m + n + 1)|m, n\rangle; \quad (9)$$

$$\frac{1}{2}(p_1^2 + x_1^2)|m\rangle = (m + \frac{1}{2})|m\rangle; \quad (10)$$

$$\frac{1}{2}(p_2^2 + x_2^2)|n\rangle = (n + \frac{1}{2})|n\rangle. \quad (11)$$

The matrix elements of Hamiltonian  $H = H_0(\mu) + \lambda V = H^0 + \mu U + \lambda V$  can be calculated as the following:

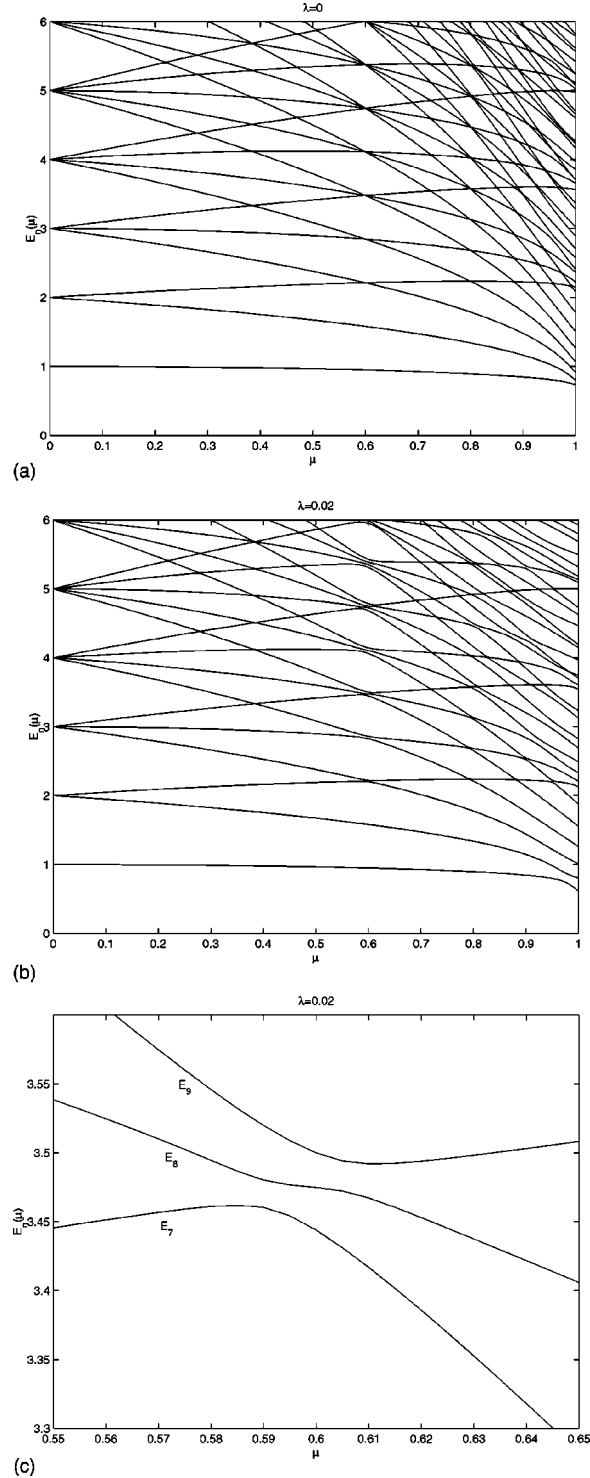
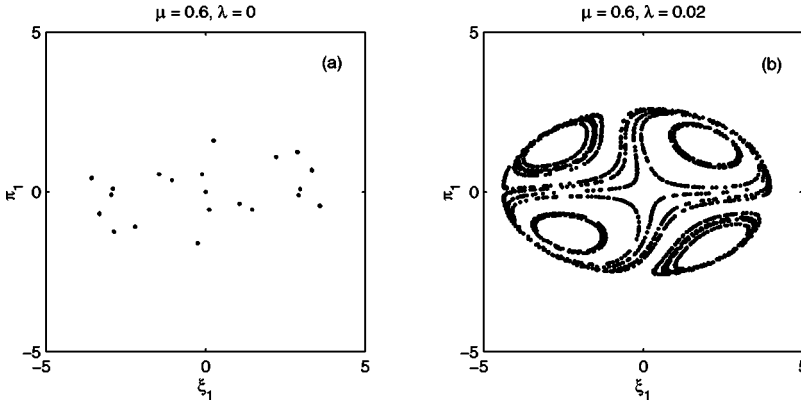


FIG. 1. (a) Energy levels of Hamiltonian  $H = H_0(\mu) + \lambda V$ , varying with  $\mu$  for  $\lambda = 0$ . The crossings of energy levels can be observed at  $\mu = 0.6$ . (For the present and following figures, the units of energy, length, and momentum are scaled by the relation  $m = \omega = \hbar = 1$ .) (b) Energy levels varying with  $\mu$  for  $\lambda = 0.02$ , splitting of the degenerate energy levels can be seen at  $\mu = 0.6$ . (c) Amplified aspect of (b) around the avoided crossing point at  $\mu = 0.6$ , the energy levels are labeled by  $E_7, E_8$ , and  $E_9$  according to their positions in the spectrum.



$$\begin{aligned}
 H_{k,l;m,n} &= \langle k,l|H|m,n\rangle \\
 &= (m+n+1)\delta_{k,m}\delta_{l,n} + \mu\langle k,l|U|m,n\rangle \\
 &\quad + \lambda\langle k,l|V|m,n\rangle.
 \end{aligned} \tag{12}$$

With the recursive formula of operators, the explicit form of the last two terms of Eq. (12) can be obtained easily. The numerical calculation is performed in a truncated subspace with  $10 \times 15$  bases, with which the result is accurate enough so long as  $\lambda$  is small (i.e.,  $\lambda < 0.1$ ). (Different numbers of the bases are also tested to convince of the convergence.)

Figure 1 shows the variation of energy levels of the system with  $\mu$  for  $\lambda = 0$  and  $0.02$ , respectively. It is noticed that in the case of  $\lambda = 0$ , most of the levels are degenerate and intersect, respectively, with each other at the point  $\mu = 0.6$ ; however, when  $\lambda = 0.02$ , due to the addition of nonintegrable perturbation  $\lambda V$ , the degenerate energy levels are split and bear the property similar to avoided crossing. Compared with the split points, the remaining parts of the energy spectrum are relatively insensitive to the nonintegrable perturbation.

Concerning the classical behavior of the system described by Eq. (4), one can see that the point  $\mu = 0.6$  corresponds to a resonant case where the ratio of classical frequencies of two independent oscillators is

$$\frac{\sqrt{1-\mu}}{\sqrt{1+\mu}} = \frac{1}{2}.$$

This indicates that the motion of the system near the point  $\mu = 0.6$  is highly unstable and sensitive to small external perturbations according to the Poincaré-Birkhoff theorem.

Poincaré section can be applied to show this classical behavior clearly. We have randomly chosen ten groups of values of  $(x_1, x_2; p_1, p_2)$  satisfying the restriction  $H = H_0(\mu) + \lambda V = \frac{5}{2}\sqrt{1-\mu} + \frac{3}{2}\sqrt{1+\mu}$  as the initial conditions (The values of parameters are  $\mu = 0.6$ ,  $\lambda = 0$ .) The restriction corresponds to the eighth energy level of the quantized system. Figures 2(a) and 2(b) show the Poincaré sections in phase plane  $\xi_1 - \pi_1$ , before and after the perturbation  $\lambda V$  is added to the system, respectively. Substantial difference can be seen between the two cases. Discrete points in Fig. 2(a) demonstrate periodic motion in contrast to the quasiperiodic motion in Fig. 2(b).

FIG. 2. Different structures of Poincaré section before and after the perturbation  $\lambda V$  is added to the system. Discrete points in (a) represent the periodic motion while the connected points in (b) represent the quasiperiodic motion.

One may ask that, what is the corresponding quantum behavior? To show this, we compute the scalar product of eigenstates of perturbed and unperturbed systems. Let  $|N\rangle$  denote the  $N$ th eigenstate of Hamiltonian  $H^0$ , and  $|N, \mu, \lambda\rangle$  of the perturbed Hamiltonian  $H = H_0(\mu) + \lambda V = H^0 + \mu U + \lambda V$ . The modulus of the product,  $|\langle N|N, \mu, \lambda\rangle|^2$  can be seen as a description of similarity between the states  $|N\rangle$  and  $|N, \mu, \lambda\rangle$ . Figure 3 shows this with  $N=8$ , corresponding to the eighth energy level in Fig. 1(a) counted from the lowest one;  $\mu$  varies continuously between 0 and 0.75. The solid line indicates  $\lambda = 0$ , the dashed line,  $\lambda = 0.02$ . It can be seen that, for  $\lambda = 0$ ,  $|\langle N|N, \mu, \lambda\rangle|^2$  varies smoothly, while an explicit gap appears around  $\mu = 0.6$  as a finite perturbation  $\lambda V$  is added. Though the corresponding eigenvalue bears very small shift around the point  $\mu = 0.6$ , the quantum state is changed dramatically as the perturbation is added.

In Fig. 4 we plot the sectional quantum phase space, the squared moduli of expansion coefficient of the state  $|N = 8, \mu, \lambda = 0.02\rangle$  by coherent states [1], that is,  $|\langle \bar{x}_1, \bar{p}_1, \bar{x}_2 = 0, \bar{p}_2 = 2|N, \mu, \lambda\rangle|^2$ . The definition of  $|\bar{x}_1, \bar{p}_1\rangle$  is

$$|\bar{x}_1, \bar{p}_1\rangle = e^{[-(1/2)|(\bar{x}_1 + i\bar{p}_1/\sqrt{2})|]} \sum_n \frac{((\bar{x}_1 + i\bar{p}_1/\sqrt{2})/\sqrt{2})^n}{\sqrt{n!}} |n\rangle,$$

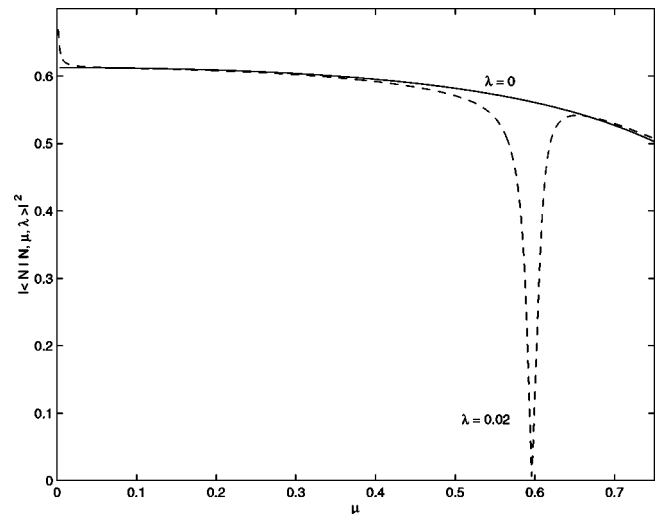


FIG. 3.  $|\langle N|N, \mu, \lambda\rangle|^2$  as a function of  $\mu$ , for  $N=8$ , gives the solid line for  $\lambda = 0$ , and the dashed line for  $\lambda = 0.02$ . An explicit gap can be seen around  $\mu = 0.6$  as the perturbation  $\lambda V$  is added.

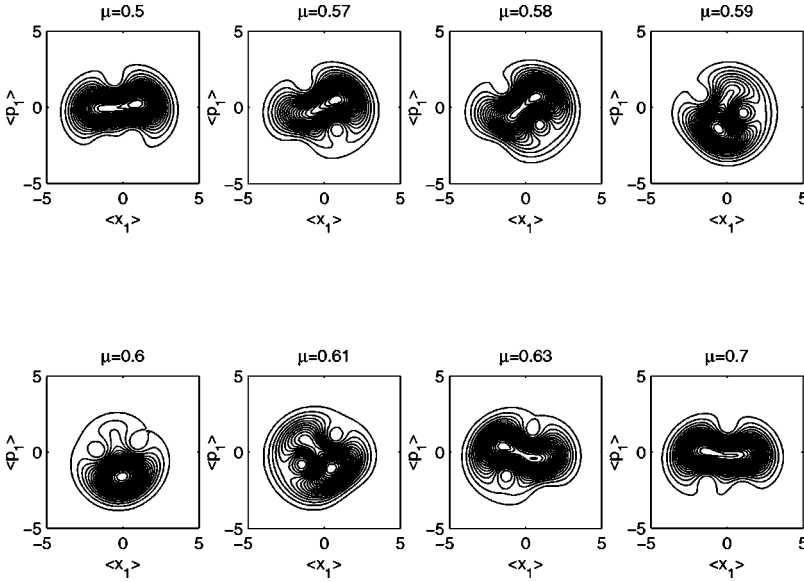


FIG. 4. Sectional quantum phase space of the state  $|N=8, \mu, \lambda=0.02\rangle$ , the visual form of the section loses and then recovers its original character as  $\mu$  crosses the degenerate point  $\mu=0.6$ .

where  $|n\rangle$  is an eigenstate defined by Eq. (10).  $|\bar{x}_1, \bar{p}_1\rangle$  is a wave packet with the least uncertainty  $\frac{1}{2}$  ( $\hbar=1$ ) and  $|\bar{x}_1, \bar{p}_1, \bar{x}_2, \bar{p}_2\rangle = |\bar{x}_1, \bar{p}_1\rangle \otimes |\bar{x}_2, \bar{p}_2\rangle$ . The result clarifies the property of the state further. It can be seen that as the parameter  $\mu$  approaches the degenerate point  $\mu=0.6$ , the visual form of the section  $|\langle \bar{x}_1, \bar{p}_1, \bar{x}_2, \bar{p}_2 = 0, \bar{p}_2 = 2|N, \mu, \lambda \rangle|^2$ , loses its original character; as  $\mu$  increases further from the point, the visual form recovers, as one can see by comparing the plots with  $\mu=0.5$  and  $\mu=0.7$ .

This behavior can be explained qualitatively by perturbation theory. Supposing  $\mu$  is smaller than 0.6 and far enough from the degeneracy point,  $|N=8, \mu, \lambda=0.02\rangle$  can be approximately expressed by the following expansion:

$$|8, \mu, \lambda=0.02\rangle = |8, \mu, \lambda=0\rangle + \sum_{N \neq 8} \frac{\lambda \langle N, \mu, \lambda=0 | V | 8, \mu, \lambda=0 \rangle}{E_8(\mu) - E_N(\mu)} |N, \mu, \lambda=0\rangle.$$

Notice that the expression is not normalized. As  $\mu$  approaches  $\mu=0.6$ , different energy levels, such as  $E_7(\mu)$ ,  $E_8(\mu)$ , and  $E_9(\mu)$ , may draw nearer, therefore the denominator  $E_8(\mu) - E_N(\mu)$  becomes smaller and the perturbation terms are amplified. Though the approximation by perturbation theory fails as  $\mu$  grows further, it seems likely that there exists a tendency that the perturbation is amplified gradually and exceeds the term  $|8, \mu, \lambda=0\rangle$  significantly, thus the character of the original state is almost lost. As  $\mu$  leaves the degeneracy point,  $E_8(\mu) - E_N(\mu)$  becomes greater, and  $|8, \mu, \lambda=0\rangle$  regains the dominant position. This is quite similar to the explanation for the property of classical resonant tori that is easily destroyed.

### III. NONPERIODICITY OF THE OBSERVABLES AT THE DEGENERATE POINTS

In the previous section we have studied the properties of quantum states, and now we tend to care about the temporal

evolution of average values of observables. Here we choose  $\xi_1 = 1/\sqrt{2}(x_1 + x_2)$ ,  $\pi_1 = 1/\sqrt{2}(p_1 + p_2)$  and monitor the temporal behavior as follows:

$$\begin{aligned} \langle \xi_1 \rangle(t) &= \langle N=8, \mu, \lambda'=0 | \exp[i(H_0 + \mu U + \lambda V)t] \\ &\quad \times \xi_1 \exp[-i(H_0 + \mu U + \lambda V)t] \\ &\quad \times |N=8, \mu, \lambda'=0\rangle \end{aligned} \quad (13)$$

and

$$\begin{aligned} \langle \pi_1 \rangle(t) &= \langle N=8, \mu, \lambda'=0 | \exp[i(H_0 + \mu U + \lambda V)t] \pi_1 \\ &\quad \times \exp[-i(H_0 + \mu U + \lambda V)t] \\ &\quad \times |N=8, \mu, \lambda'=0\rangle. \end{aligned} \quad (14)$$

In the above expressions,  $\mu$  is an adjustable parameter, and it takes the same value in the quantum states  $|N=8, \mu, \lambda'=0\rangle$  as well as in the operators  $\exp[-i(H_0 + \mu U + \lambda V)t]$ . It should be emphasized that  $\lambda'$  in the quantum states is fixed at  $\lambda'=0$ , while  $\lambda$  in the operators  $\exp[-i(H_0 + \mu U + \lambda V)t]$  is fixed at  $\lambda=0.02$ . The significance of the expressions is that, the average value of observable  $\xi_1$  or  $\pi_1$  starts from an unperturbed state (i.e.,  $\lambda'=0$ ), while it is evolved by a temporal evolution operator with perturbed Hamiltonian  $H = H_0(\mu) + \lambda V$ .

Now we estimate the temporal behavior of Eqs. (13) and (14). First, for Eq. (13), in the interaction picture it can be written as

$$\begin{aligned} \langle \xi_1 \rangle(t) &= \langle N=8, \mu, \lambda'=0 | \exp[i(H_0 + \mu U + \lambda V)t] \\ &\quad \times \xi_1 \exp[-i(H_0 + \mu U + \lambda V)t] \\ &\quad \times |N=8, \mu, \lambda'=0\rangle \\ &= \langle N=8, \mu, \lambda'=0, I | \exp[i(H_0 + \mu U)t] \\ &\quad \times \xi_1^S \exp[-i(H_0 + \mu U)t] \\ &\quad \times |N=8, \mu, \lambda'=0, I\rangle, \end{aligned} \quad (15)$$

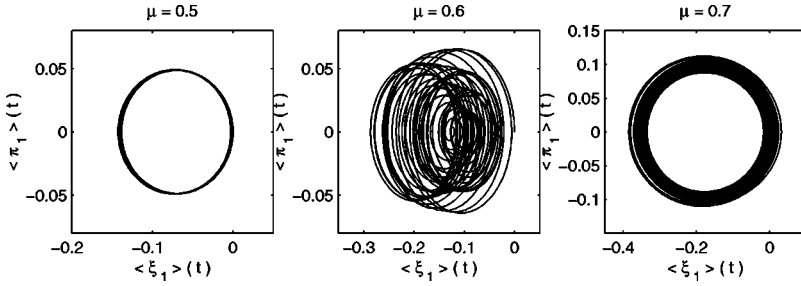


FIG. 5. Trajectory of average values on the phase plane  $\langle \xi_1 \rangle - \langle \pi_1 \rangle$  for  $\mu = 0.5, 0.6$ , and  $0.7$ , respectively. In the cases away from the resonance value, i.e.,  $\mu = 0.5, 0.7$ , the motion is periodic or quasiperiodic. In the resonant case,  $\mu = 0.6$ , the motion is totally aperiodic.

where  $|N=8, \mu, \lambda'=0, I\rangle$  is the corresponding quantum state of  $|N=8, \mu, \lambda'=0\rangle$  in the interaction picture, satisfying

$$\begin{aligned} |N=8, \mu, \lambda'=0, I\rangle &= \exp[i(H_0 + \mu U)t] \\ &\times \exp[-i(H_0 + \mu U + \lambda V)t] \\ &\times |N=8, \mu, \lambda'=0\rangle; \end{aligned}$$

and  $\exp[i(H_0 + \mu U)t] \xi_1^S \exp[-i(H_0 + \mu U)t] = \xi_1^I(t) = \xi_1^H(t)$ ,  $\xi_1^S = \xi_1$  is the operator in the Schrödinger's picture, and  $\xi_1^I(t)$ ,  $\xi_1^H(t)$  are the operators in the interaction and the Heisenberg picture respectively. The evolution of  $\xi_1^H(t)$  or  $\xi_1^I(t)$  is formally identical to the classical case when the Hamiltonian is  $H = H_0 + \mu U$ ; thus we obtain

$$\begin{aligned} &\exp[i(H_0 + \mu U)t] \xi_1^S \exp[-i(H_0 + \mu U)t] \\ &= \xi_1^S \cos(t\sqrt{1-\mu}) + \frac{\pi_1^S}{\sqrt{1-\mu}} \sin(t\sqrt{1-\mu}). \end{aligned} \quad (16)$$

Substituting Eq. (16) into Eq. (15), we get

$$\begin{aligned} \langle \xi_1 \rangle(t) &= \langle N=8, \mu, \lambda'=0, I | \exp[i(H_0 + \mu U)t] \\ &\times \xi_1^S \exp[-i(H_0 + \mu U)t] | N=8, \mu, \lambda'=0, I \rangle \\ &= \langle N=8, \mu, \lambda'=0, I | \xi_1^S | N=8, \mu, \lambda'=0, I \rangle \\ &\times \cos(t\sqrt{1-\mu}) + \frac{1}{\sqrt{1-\mu}} \\ &\times \langle N=8, \mu, \lambda'=0, I | \pi_1^S | N=8, \mu, \lambda'=0, I \rangle \\ &\times \sin(t\sqrt{1-\mu}). \end{aligned} \quad (17)$$

Notice that the coefficients  $\langle N=8, \mu, \lambda'=0, I | \xi_1^S | N=8, \mu, \lambda'=0, I \rangle$  and  $1/\sqrt{1-\mu} \langle N=8, \mu, \lambda'=0, I | \pi_1^S | N=8, \mu, \lambda'=0, I \rangle$  are time dependent, therefore, in a sense, the temporal evo-

lution of  $\langle \xi_1 \rangle(t)$  can be seen as a tuned sinusoidal wave. The angular frequency  $\sqrt{1-\mu}$  of the average value is just the angular frequency of classical motion when  $\lambda = 0$ .

Due to the complexity of the term  $\langle N=8, \mu, \lambda'=0, I | \xi_1^S | N=8, \mu, \lambda'=0, I \rangle$  and  $1/\sqrt{1-\mu} \langle N=8, \mu, \lambda'=0, I | \pi_1^S | N=8, \mu, \lambda'=0, I \rangle$ , a numerical method needs to be applied to see the behavior of the observables. Figure 5 shows the trajectories of the average values in the phase plane  $\langle \xi_1 \rangle - \langle \pi_1 \rangle$ . Here  $\mu$  has been selected for three different values: the first one is  $\mu = 0.5$ , smaller than the value corresponding to the classical resonance case; the second one is  $\mu = 0.6$ , which is just the resonance case as well as the degeneracy point for the quantum system; the third one is  $\mu = 0.7$ . It can be seen that for  $\mu = 0.5$  and  $\mu = 0.7$ , which are away from the resonance value, the motion of the average values is periodic or at least quasiperiodic; however, at the point  $\mu = 0.6$  the motion is obviously aperiodic.

In Fig. 6, we plot the logarithmic power spectra  $\log_{10}(P_r)$  [2,9] to demonstrate the periodicity of  $\langle \xi_1 \rangle(t)$ . The definition of  $P_r$  is

$$P_r(f) = \frac{P(f)}{\min\{P(f)\}},$$

where  $P(f)$  is the fast Fourier transform of the time series of  $\langle \xi_1 \rangle(t)$ ,  $f$  stands for the frequency, and  $\min\{P(f)\}$  is the minimum in the power spectrum  $P(f)$ .

In Fig. 6, it can be seen that for  $\mu = 0.5$  the spectrum is of a periodic or quasiperiodic type. The relevant frequencies observed in the spectrum are  $\sqrt{1-\mu}/2\pi \approx 0.113$ , which is equal to the classical frequency of  $\xi_1(t)$ , along with all the multiples  $2\sqrt{1-\mu}/2\pi, 3\sqrt{1-\mu}/2\pi, \dots; \sqrt{1+\mu}/2\pi \approx 0.195$ , which is the frequency of classical motion of  $\xi_2(t)$ , along with all the multiples  $2\sqrt{1+\mu}/2\pi, 3\sqrt{1+\mu}/2\pi, \dots$ ; apart from these frequencies, we can also observe the other beat frequencies:  $\sqrt{1+\mu}/2\pi - \sqrt{1-\mu}/2\pi \approx 0.0824$ ,  $2\sqrt{1-\mu}/2\pi - \sqrt{1+\mu}/2\pi \approx 0.0302$ ,  $\sqrt{1-\mu}/2\pi + \sqrt{1+\mu}/2\pi \approx 0.307 \dots$ . The existence of all the beat frequencies arises

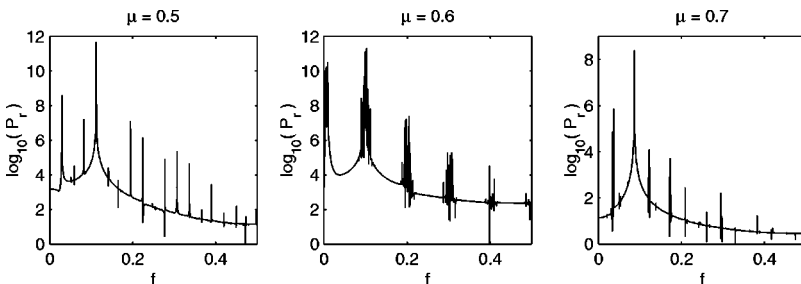


FIG. 6. The logarithmic power spectra  $\log_{10}(P_r)$  of  $\langle \xi_1 \rangle(t)$ . For  $\mu = 0.5$  and  $\mu = 0.7$  the spectra are of periodic or quasiperiodic type, i.e., there only exist discrete peaks in the spectra; for  $\mu = 0.6$ , a series of resonant bands can be seen around the frequencies of classical motion.

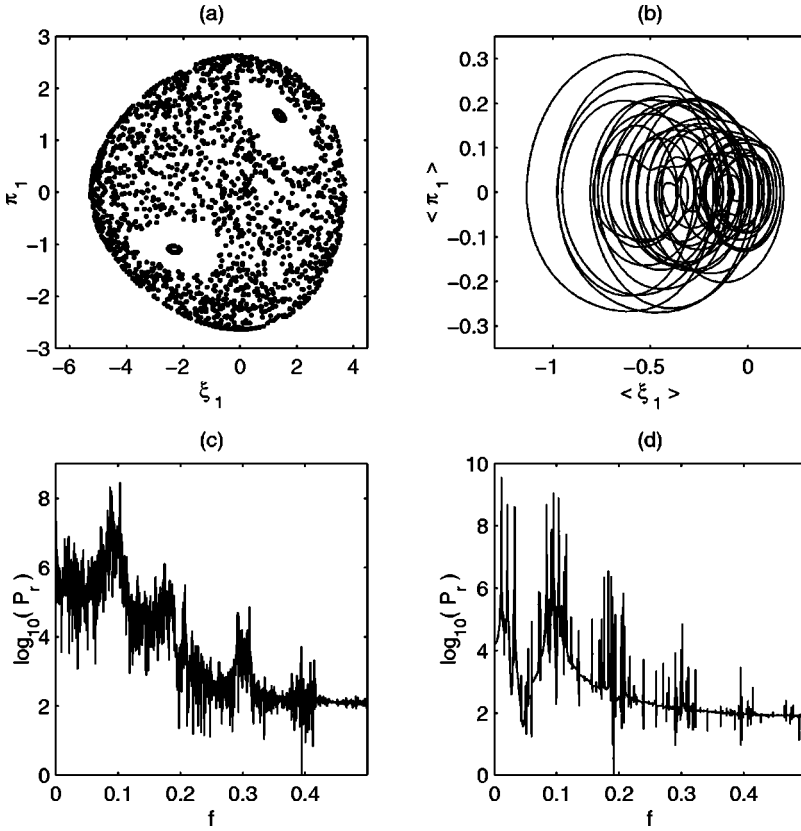


FIG. 7. A comparison between the classical and the quantum-mechanical motion for  $\mu=0.6$  and  $\lambda=0.06$ . The Poincaré section of classical chaotic motion is shown in (a); the quantum motion of the trajectory in phase plane  $\langle \xi_1 \rangle - \langle \pi_1 \rangle$  is shown in (b). Power spectrum of classical chaotic motion (c) and quantum motion (d) are also shown. Chaoticlike spectrum of quantum motion can be seen.

from the nonlinearity in the expression of Eq. (17); this property is similar to that of nonlinear wave systems. Beyond the resonance point or  $\mu=0.7$ , the property of the power spectrum is quite similar to that of  $\mu=0.5$ , indicating that the motion is also periodic or quasiperiodic.

Now we turn to the resonance case  $\mu=0.6$ . The behavior is totally different from the previous ones. Since  $\sqrt{1-\mu}/\sqrt{1+\mu}=\frac{1}{2}$ , or  $2\sqrt{1-\mu}=\sqrt{1+\mu}$ , we would expect that the positions of the multiples of  $\sqrt{1-\mu}$ ,  $\sqrt{1+\mu}$  and  $|m\sqrt{1-\mu} \pm n\sqrt{1+\mu}|$  should overlap each other. However, in the spectrum, we can see many frequencies around the multiples of  $\sqrt{1-\mu}$ . These multifrequencies with very small difference can be explained as the energy shifts or the avoided crossing due to the introduction of nonintegrable perturbation.

One can expect that, as the perturbation strength  $\lambda$  increases, the energy-level shift becomes greater and the bands of frequencies around the multiples of  $\sqrt{1-\mu}/2\pi$  become broader and overlap each other; the spectrum thus becomes chaoticlike one. In Fig. 7 we compare the power spectra of classical chaotic motion with the corresponding quantum case for  $\mu=0.6$  and  $\lambda=0.06$ . As one can see, both spectra bear the same kind of structure. There are peaks at the multiples of classical frequencies while there also exists noise-like background, although in the spectrum of the quantum system, the number of noise-like peaks is fewer than in the classical system, which is probably due to the fact that the energy is not so high and chaos is suppressed by the quantum effect.

#### IV. DISCUSSION AND CONCLUSION

In this paper, a quasi-integrable quantum system is established and studied, the sensitivity behavior at the degeneracy points (or the avoided crossing points of energy levels) is demonstrated. We have seen that the quantum system is highly sensitive at the degeneracy points.

According to the semiclassical approximation, for a two-dimensional quasi-integrable system, the condition of nonlinear resonance is [3].

$$n_1\omega_1 + n_2\omega_2 = n_1 \frac{\partial H^0}{\partial I_1} + n_2 \frac{\partial H^0}{\partial I_2} = 0.$$

One can find that the above condition corresponds to the quantum energy-level degeneracy of the system, that is to say, the energy-level degeneracy is related to the resonant tori of classical motion. The unperturbed system we have discussed is a special case where the degeneracy corresponds to the classical resonant tori directly without invoking semiclassical analysis. This provides us with a simple and straight way to compare the classical and the quantum motion for the system. With this in our minds, we further studied the temporal evolution of observed quantities. In accordance with the sensitivity, we find that the observables evolve aperiodically and chaoticlike behavior can be observed at the point where degeneracy or avoided crossing happens. The transition from regular to chaoticlike motion is likely through the following process:

- (1) Degeneracies take place;

(2) as perturbation is added, a strong resonance occurs between the energy levels, the original degenerate frequencies are split;

(3) as the perturbation is strengthened, the frequencies are split further, and different resonant bands of the frequencies overlap, the spectrum becomes chaoticlike and so does the motion of the average value of observables.

We need to point out that since the expressions of the average value of observables are nonlinear, much nonlinear behavior can be displayed in quantum systems; the beat fre-

quencies we observe in the power spectra are just good examples. The nonperiodicity at the degenerate points can also be attributed to the nonlinear effect.

#### ACKNOWLEDGMENTS

This work was supported by the National Natural Science Foundation of China under Grant No. 19975006, the Special Funds for Major State Basic Research Projects, and RFDP.

- 
- [1] L.E. Reichl, *The Transitions to Chaos in Conservative Classical Systems: Quantum Manifestations* (Springer-Verlag, New York, 1992).
- [2] E. Ott, *Chaos in Dynamical Systems* (Cambridge University, Cambridge, 1993).
- [3] Gong-ou Xu, *Chaotic Motions in Quantum Systems* (Shanghai Scientific and Technical Publishers, Shanghai, China, 1995) (in Chinese).
- [4] Gong-ou Xu and Quan-lin Jie, Phys. Lett. A **197**, 121 (1995).
- [5] Kaifen He and Gang Hu, Phys. Lett. A **190**, 38 (1994).
- [6] M. Latka, P. Grigolini, and B.J. West, Phys. Rev. A **50**, 1071 (1994).
- [7] V.I. Arnold, *Mathematical Methods of Classical Mechanics* (Springer-Verlag, New York, 1978).
- [8] Qing-Rong Zheng, Gang Su, and De-Hai Zhang, Phys. Lett. A **212**, 138 (1996).
- [9] S. Neil Rasband, *Chaotic Dynamics of Nonlinear Systems* (Wiley, New York, 1989).
- [10] F. Simmel and M. Eckert, Physica D **97**, 517 (1996).
- [11] D. Kusnezov and C.H. Lewenkopf, Phys. Rev. E **53**, 2283 (1996).
- [12] Z. Lin and M. Goda, Phys. Rev. E **55**, 2632 (1997).
- [13] U. Schwengelbeck and F.H.M. Faisal, Phys. Lett. A **199**, 281 (1995).
- [14] R.H. Parmenter and R.W. Valentine, Phys. Lett. A **201**, 1 (1995).
- [15] R.H. Parmenter and R.W. Valentine, Phys. Lett. A **227**, 5 (1997).
- [16] G. Iacomelli and M. Pettini, Phys. Lett. A **212**, 29 (1996).
- [17] S. Sengupta and P.K. Chattaraj, Phys. Lett. A **215**, 119 (1996).
- [18] H. Frisk, Phys. Lett. A **227**, 139 (1997).
- [19] A. Farini, S. Boccaletti, and F.T. Arecchi, Phys. Rev. E **53**, 4447 (1996).
- [20] G.G. de Polavieja, Phys. Lett. A **220**, 303 (1996).